

2015

Bridge Structural Condition Assessment using 3D Imaging

Simon Laflamme

Iowa State University, laflamme@iastate.edu

Yelda Turkan

Iowa State University

Liangyu Tan

Iowa State University, tan@iastate.edu

Follow this and additional works at: http://lib.dr.iastate.edu/ccee_conf

 Part of the [Civil Engineering Commons](#), [Construction Engineering and Management Commons](#), and the [Transportation Engineering Commons](#)

Recommended Citation

Laflamme, Simon; Turkan, Yelda; and Tan, Liangyu, "Bridge Structural Condition Assessment using 3D Imaging" (2015). *Civil, Construction and Environmental Engineering Conference Presentations and Proceedings*. 33.
http://lib.dr.iastate.edu/ccee_conf/33

This Conference Proceeding is brought to you for free and open access by the Civil, Construction and Environmental Engineering at Iowa State University Digital Repository. It has been accepted for inclusion in Civil, Construction and Environmental Engineering Conference Presentations and Proceedings by an authorized administrator of Iowa State University Digital Repository. For more information, please contact digirep@iastate.edu.

Bridge Structural Condition Assessment using 3D Imaging

Simon Laflamme
Department of Civil, Construction and Environmental Engineering
Iowa State University
416A Town Engineering
Ames, IA 50011-3232
laflamme@iastate.edu

Yelda Turkan
Department of Civil, Construction and Environmental Engineering
Iowa State University
428 Town Engineering
Ames, IA 50011-3232
yturkan@iastate.edu

Liangyu Tan
Department of Civil, Construction and Environmental Engineering
Iowa State University
427 Town Engineering
Ames, IA 50011-3232
tan@iastate.edu

ABSTRACT

Objective, accurate, and fast assessment of bridge structural condition is critical to timely assess safety risks. Current practices for bridge condition assessment rely on visual observations and manual interpretation of reports and sketches prepared by inspectors in the field. Visual observation, manual reporting and interpretation has several drawbacks such as being labor intensive, subject to personal judgment and experience, and prone to error. Terrestrial laser scanners (TLS) are promising sensors to automatically identify structural condition indicators, such as cracks, displacements and deflected shapes, as they are able to provide high coverage and accuracy at long ranges. However, there is limited research conducted on employing TLS to detect cracks for bridge condition assessment, which mainly focused on manual detection and measurements of cracks, displacements or shape deflections from the laser scan point clouds. TLS is an advance 3D imaging technology that is used to rapidly measure the 3D coordinates of densely scanned points within a scene. The data gathered by a TLS is provided in the form of 3D point clouds with color and intensity data often associated with each point within the cloud. This paper proposes a novel adaptive wavelet neural network (WNN) based approach to automatically detect concrete cracks from TLS point clouds for bridge structural condition assessment. The adaptive WNN is designed to self-organize, self-adapt, and sequentially learn a compact reconstruction of the 3D point cloud. The architecture of the network is based on a single-layer neural network consisting of Mexican hat wavelet functions. The approach was tested on a cracked concrete specimen. The preliminary experimental results show that the proposed approach is promising as it enables detecting concrete cracks accurately from TLS point clouds. Using the proposed method for crack detection would enable automatic and remote assessment of bridge condition. This would, in

turn, result in reducing costs associated with infrastructure management, and improving the overall quality of our infrastructure by enhancing maintenance operations.

Key words: laser scanning—bridge condition assessment—crack detection—wavelets—neural networks

INTRODUCTION

The majority of bridge condition assessments in the U.S. are conducted by visual inspection, during which a printed checklist is filled by trained inspectors. An inspector must correctly identify the type and location of each element being inspected, document its distress, manually record this information in the field and then transcribe that information to the bridge evaluation database after arriving back at his/her office. This is a complex and time-consuming set of responsibilities which are prone to error.

Terrestrial laser scanners (TLS) are promising sensors for documenting as-built condition of infrastructure (Hajian and Brandow, 2012), and they have already been utilized by a number of state DOTs for this purpose at the project planning phase. Furthermore, TLS technology has been shown to be effective identifying structural condition indicators, such as cracks, displacements and deflected shapes (Park et al. 2007; Olsen et al. 2009; Werner and Morris, 2010; Meral 2011; Wood et al. 2012), as they are able to provide high coverage and accuracy at long ranges. However, there is limited research conducted on employing TLS to detect cracks for bridge condition assessment, which mainly focused on manual detection and measurements of cracks, displacements or shape deflections from the laser scan point clouds (Chen 2012; Chen et al. 2014; Olsen et al. 2013).

The research presented in this paper attempts to automatically detect cracks from TLS point clouds (Olsen et al. 2009; Anil et al. 2013; Adhikari et al. 2013; Mosalam et al. 2013) for bridge structural condition assessment. TLS is an advance imaging technology that is used to rapidly measure the 3D coordinates of densely scanned points within a scene (Fig. 1(a)). The data gathered by a TLS is provided in the form of 3D point clouds with color and intensity data often associated with each point within the cloud. Point cloud data can be analyzed using computer vision algorithms (Fig. 1(b)) to detect structural conditions (Fig 1(c)).

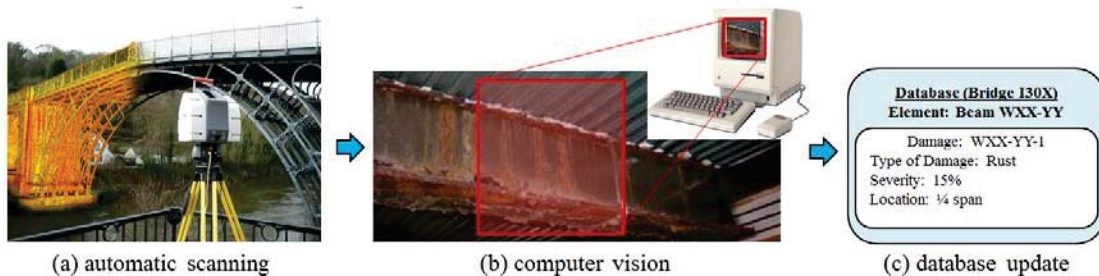


Figure 1. Research Vision

In its raw format, TLS point cloud data contains significant number of data points that is unstructured, densely and non-uniformly distributed (Meng et al. 2013). Therefore, in machine learning community, substantial effort has been put in reconstructing 3D shapes from point

clouds. Popular reconstruction methods include the utilization of Splines (Gálvez & Iglesias 2012) and partial differential equations (PDE) (Wang et al. 2012), seen as an improvement over Splines in terms of numbers of parameters. Neural networks have also been proposed, and demonstrated as superior to PDE-based methods in (Barhak & Fisher 2001).

The overarching goal of this research is to detect 3D shapes from point clouds real-time while scanning on-site. However, there exist critical challenges in designing a shape reconstruction algorithm for real-time adaptive scanning, namely:

- The algorithm must adapt sequentially to enable adaptive scanning.
- The representations must be compact to reduce demand on memory. A compact representation can also facilitate queries over a large database, particularly useful in extracting prior information in the case of sequential training.
- The number of parameters must remain low to accelerate computational speed. A high number of parameters would result in a substantial lag in the parameterization process.
- The algorithm must be robust with respect to noise in data, which can be substantial with TLS-based technologies.

Neural networks have been proposed as candidates for providing robust and compact representations. In particular, Radial Basis Functions (RBF) neural networks have been applied to the problem of shape reconstruction (Bellocchio et al. 2013). Compared against traditional types of neural networks, they provide a better approximation, convergence speed, optimality in solution and excellent localization (Suresh et al. 2008). Furthermore, they can be trained faster when modeling nonlinear representations in the function space (Howlett 2001). Recent work has been published in utilizing sequential RBF networks for reconstructing surfaces from point clouds (Meng et al. 2013). A self-organizing mapping (SOM) (Kohonen 2001) architecture was used to optimize node placement, and the algorithm provided good accuracy with minimum number of nodes.

The authors have developed a sequential adaptive RBF neural network for real-time learning of nonlinear dynamics (Laflamme & Connor 2009), and returned similar conclusions where the network showed better performance with respect to traditional neural networks. They also designed wavelet neural networks (WNN) for similar applications in (Laflamme et al. 2011, Laflamme et al. 2012). WNN are also capable of universal approximation, as shown in (Zhang & Benveniste 1992). This particular neural network has also been demonstrated as capable to learn dynamics on-the-spot, without prior knowledge of the underlying dynamics and architecture of the input space.

The study presented in this paper proposes a novel adaptive wavelet neural network (WNN) based approach to automatically detect concrete cracks from TLS point clouds for bridge structural condition assessment. The adaptive WNN is designed to self-organize, self-adapt, and sequentially learn a compact reconstruction of the 3D point cloud. The approach was tested on a cracked concrete specimen, and it successfully reconstructed 3D laser scan data points as wavelet functions in a more compact format, where the concrete crack was easily identified. This is a significant improvement over previous TLS based crack detection methods as it does not require a priori knowledge about the crack or the 3D shape of the object being scanned. It also enables to process 3D point cloud data faster and detect cracks automatically. Furthermore, since it is designed to self-organize, self-adapt and sequentially learn a compact reconstruction of the 3D point cloud, it can easily be adapted for real-time scanning in the field, which will be investigated in the future using the adaptive WNN approach presented in this paper.

BACKGROUND

Terrestrial Laser Scanning (TLS) Technology

Terrestrial Laser Scanning (TLS) – also known as Light Detection and Ranging (LiDAR) – enables direct acquisition of 3D coordinates from the surface of a target object or scene that are visible from the laser scanner's viewpoint (Alba et al. 2011; Vosselman and Maas 2013; Xiong et al. 2013). TLS is based on either time-of-flight (TOF) or phase-based technology to collect range (x, y, z) and intensity data of objects in a scene. The two technologies differ in calculating the range, while both acquire each range point in the equipment's spherical coordinate frame by mounting a laser on a pan-and-tilt unit that provides the spherical angular coordinates of the point. TOF scanners emit a pulse of laser light to the surface of the target object or scene and calculate the distance to the surface by recording the round trip time of the laser light pulse. Phase based scanners measure phase shift in a continuously emitted and returned sinusoidal wave. Both types of TLS achieve similar point measurement accuracies. They differ in scanning speed and maximum scanning range. Typically, phase-based TLS achieve faster data acquisition (up to one million points per second), while TOF-based TLS enables collecting data from longer ranges (up to a kilometre).

TLS implementation in the AEC-FM Industry

Laser scanning technology enables capturing comprehensive and very accurate three-dimensional (3D) data for an entire construction scene using only a few scans (Cheok et al. 2002). Among other 3D sensing technologies, laser scanning is the best adapted technology for capturing the 3D status of construction projects and condition of infrastructure accurately and efficiently. In a study by Greaves and Jenkins (2007), it is shown that the 3D laser scanning hardware, software, and services market has grown exponentially in the last decade, and the Architecture, Engineering, Construction and Facilities Management (AEC-FM) industry is one of its major customers. This shows that owners, decision makers and contractors are aware of the potential of using this technology for capturing the 3D as-built status of construction projects and condition of infrastructure. However, laser scanners' current adoption rate is very low despite their tremendous benefits. The major reasons are related to the big size of data they produce and the long data processing time required.

Laser scanners can output extremely high resolution models, but at a much larger file size and processing time (Boehler and Marbs, 2003). Despite the remarkable accuracy and benefits, laser scanners' current adoption rate in the AEC-FM industry is still low, mainly because of the data acquisition and processing time and data storage issues. Full laser scanning requires significant amount of time. Depending on the size of the site, it can take days for large scale high-resolution shots. Accordingly, resulting data file sizes are typically very large (e.g., a single high resolution scan file size could be a couple of gigabytes or much larger). Therefore, data storage and processing are the two biggest factors for the low adoption rates of laser scanners in the AEC-FM industry.

Thus, there is a need for advanced algorithms that enable automated 3D shape detection from low resolution point clouds during data collection. This would improve project productivity as well as safety by reducing the amount of time spent on-site. Importantly, practical applications of the developed algorithms to field laser scanners will be straightforward since commercially available laser scanners on the market are generally programmable (Trimble Inc. 2015).

RESEARCH METHODOLOGY: ADAPTIVE WAVELET NETWORK

An adaptive wavelet neural network (WNN) has been designed to sequentially learn a compact reconstruction of the 3D point cloud. The architecture of the WNN is based on a single-layer neural network, as illustrated in Fig. 2, consisting of h *Mexican Hat* wavelets centered at μ_i , with a bandwidth σ_i where each function (or node) ϕ_i can be written as below:

$$\phi_i(\zeta) = \left(1 - \frac{\|\zeta - \mu\|^2}{\sigma^2}\right) e^{-\frac{\|\zeta - \mu\|^2}{\sigma^2}} \quad \text{for } i = 1, 2, \dots, h \quad (1)$$

The wavelet network maps the z_j coordinate of point $\zeta_j = [x_j, y_j]$ using the following function:

$$\tilde{z}_j = \sum_{i=1}^h \gamma_i \phi_i(x_j, y_j) \quad (2)$$

where γ_i are function weights, and the tilde denotes an estimation.

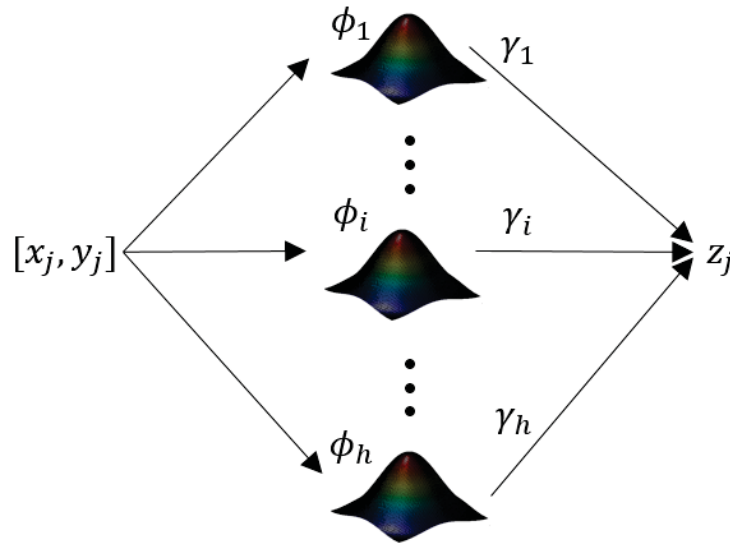


Figure 2. Single-layer architecture of the wavelet network

The network is self-organizing, self-adaptive, and sequential. The self-organizing feature consists of the capability to add functions at sparse locations. This is done following Kohonen's Self-Organizing Mapping Theory (Kohonen 2001). The self-adaptive feature consists of adapting the network parameters σ and γ to learn the compact representation. Lastly, the sequential feature refers to the capability of the network to learn at representation while scanning is occurring, in a sequential way, in opposition to a batch process. This sequential capability would be used to interact with the 3D scanner in real-time.

The wavelet network algorithm is as follows. First, a new point ζ_j is queried from the scanner, along with its associated z_j . The shortest Euclidean distance is computed between the location

of the new point ζ_j and the center of the existing functions μ_i for $i = 1, 2, \dots, h$. If the shortest distance is greater than a user-defined threshold λ , a new function is added at $\mu_{h+1} = \zeta_j$ and the number of functions increases by 1. Note that this threshold decreases with decreasing bandwidth σ_i , which allows the creation of denser regions where the network resolution is higher. The weight of the new function is taken as $\gamma_{h+1} = z_j$. Second, if no new function is added, the estimate \tilde{z}_j is compared against the value z_j , and the network error $e = \tilde{z}_j - z_j$ is computed. Third, the network parameters σ_i and γ_i are adapted using the backpropagation method (Laflamme *et al.* 2012):

$$\dot{\xi} = -\Gamma_{\xi} \left(\frac{\delta Z}{\delta \xi} \right) e \quad (3)$$

where $\xi = [\sigma, \gamma]$, and Γ_{ξ} are positive constants representing the learning rate of the network.

EXPERIMENTS AND PRELIMINARY RESULTS

The adaptive wavelet network has been validated on a cracked concrete specimen. The specimen was scanned using a Trimble TX5 phase-based TLS on a region limited to 50 by 65 mm² to focus the study on the algorithm itself. A total of 8170 points have been generated. The specimen is shown in Fig. 3, along with a zoom on the limited region (Fig. 3(b)). Fig. 3 (b) shows the crack that runs through the region with a wider region (along the first 35.1 mm from the bottom), and a smaller damage geometry along 9.8 mm and after.

Fig. 4 shows a typical fitting result obtained using 59 nodes. The compact representation provides a good fit of the 3D point cloud, and includes the damage feature. A study was conducted on the accuracy of the representation as a function of the number of nodes in the network, by changing the parameter λ while keeping all other network parameters constant. The accuracy was measured in terms of the root means square (RMS) error. Fig. 5 is a plot of the RMS error as a function of the number of nodes. It also shows the relative computing time versus the network size. In this case, there is a region in which the algorithm provides an optimal representation in term of RMS error. The decrease in performance for a higher number of nodes can be attributed to the network parameters that become mistuned. In particular, when more nodes are allowed in the network and the initial bandwidth is large, one would expect a relatively higher training period to obtain an acceptable level of accuracy. The relative computing time changes linearly with the number of nodes in the network.

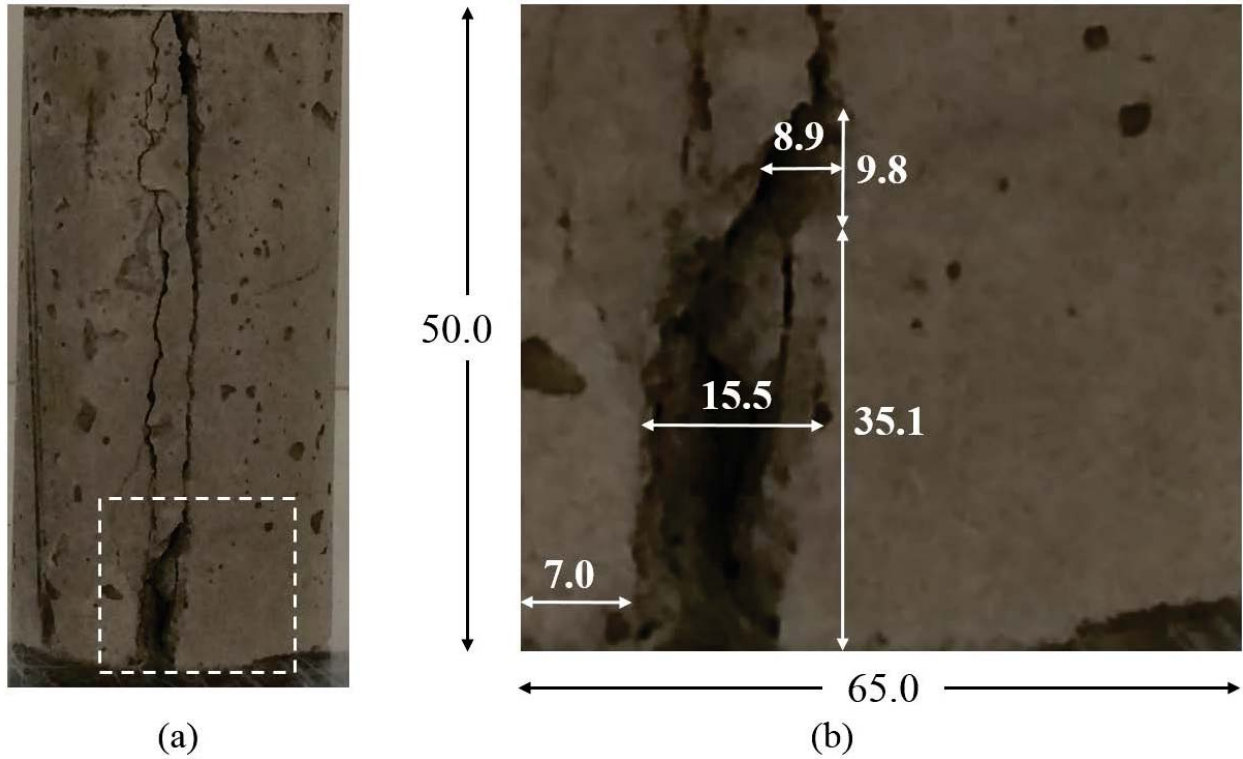


Figure 3. (a) Specimen (scanned region shown by the dashed rectangle); and (b) zoom on the scanned region (distances in mm).

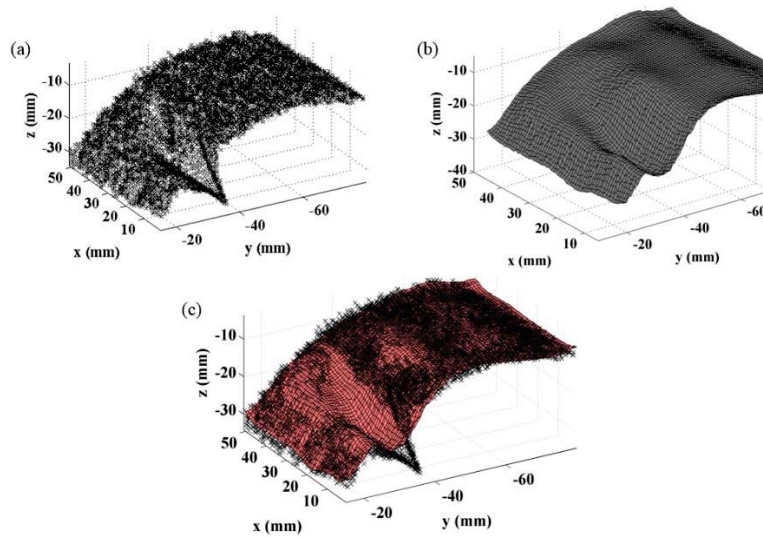


Figure 4. (a) Point cloud; (b) Compact representation; and (c) Overlap of point cloud and representation.

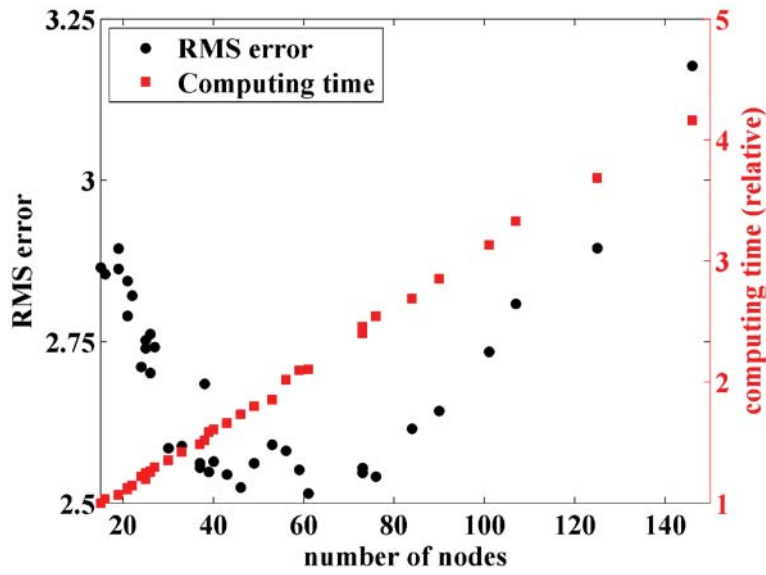


Figure 5. RMS error and relative computing time versus wavelet network size.

While the wavelet network provides an accurate representation of the 3D point cloud, it should be also capable of extracting key features, such as damage. With this particular example, an attempt was made to automatically localize the damage and determine its severity. The strategy consists of identifying regions of wavelets (or nodes) of lower bandwidths, which would indicate a region of higher resolution, thus the location of a more complex feature (a crack, in this case). Fig. 6(a) is a wavelet resolution map, which is obtained by computing the average wavelet bandwidth within a region of the representation. Dark blue areas indicate a high resolution region, while dark red areas represent low resolution regions. The damage is approximately localized using this strategy. Next, the crack length and width were estimated by evaluating the maximum distances along the x- and y-axes within a group of wavelets of low bandwidth. Fig. 6(b) is a plot of the computed crack length and width as a function of the number of nodes. The approximate crack length is more accurately determined for networks created with a large number of nodes, but yet yields to an acceptable approximation. The estimated crack width increases with increasing number of nodes. This is explained by the presence of a high resolution region around the coordinate $[-20, 20]$, shown in Fig. 6(a), that is perceived as a crack. A representation created with a large number of functions may over-fit the 3D point cloud.

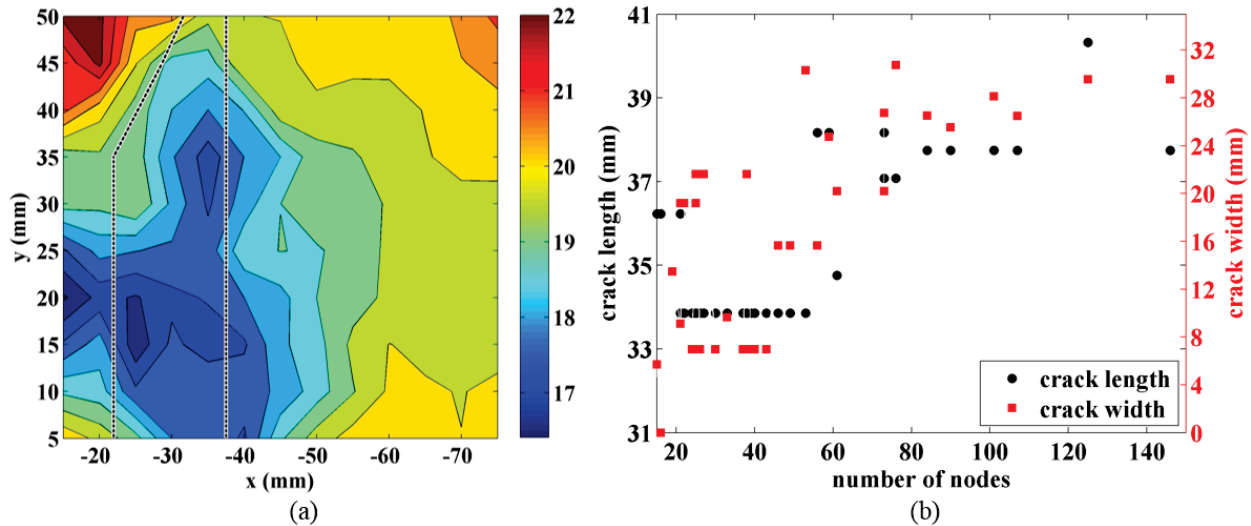


Figure 6. (a) Wavelet resolution map showing the average wavelet bandwidths for a representation using 59 nodes (the approximate crack region is shown within the black-dashed region); and (b) Identified crack length and width based on wavelet resolutions.

CONCLUSIONS

A strategy to sequentially construct a compact representation of a 3D point cloud has been presented. The representation is wavelet network capable of self-organization, self-adaptation, and sequential learning. It can be utilized to transform thousands of 3D point cloud data obtained from a TLS or LiDAR into a small set of functions. The proposed wavelet network has been demonstrated on a cracked cylindrical specimen. It was shown that the algorithm was capable of replacing a set of 8170 3D coordinates into a set of 59 functions while preserving the key features of the scan data, which included a crack. By looking at local regions of high-resolution wavelets, it is possible to localize these features, and estimate their geometry. While the promise of automatic damage detection has been demonstrated, the development of more complex algorithms in future work could lead to more accurate numerical localization and estimation of damage.

ACKNOWLEDGMENTS

This research is funded by Midwest Transportation Center (Award# 011296-00014). The authors would like to thank Ahmad Abu-Hawash, Justin Spencer, and Michael Todsén from Iowa DOT for their continuous support by providing us with data, and for sharing their expertise and experience during this project. Any opinions, findings, conclusions, or recommendations expressed in this paper are those of the authors and do not necessarily reflect the views of Midwest Transportation Center or Iowa DOT.

REFERENCES

- Alba M.I., Barazzetti L., Scaioni M. Rosina E., and Previtali M. Mapping infrared data on terrestrial laser scanning 3D models of buildings, *Remote Sensing*, 3(9): 1847–1870, 2011.
- Anil E.B., Akinci B., Garrett J.H., Kurc O. (2013). Characterization of laser scanners for detecting cracks for post-earthquake damage inspection. *Proceedings of the International Symposium on Automation and Robotics in Construction and Mining*, IAARC, pp 313-320.

- Adhikari, R. S., Zhu, Z., Moselhi, O., & Bagchi, A. (2013). Automated Bridge Condition Assessment with Hybrid Sensing. *Proceedings of the International Symposium on Automation and Robotics in Construction and Mining*, IAARC, pp.1263-1270.
- Barhak, J., & Fischer, A. (2001). Parameterization and reconstruction from 3D scattered points based on neural network and PDE techniques. *Visualization and Computer Graphics, IEEE Transactions on*, 7(1), 1-16.
- Bellocchio, F., Borghese, N. A., Ferrari, S., & Piuri, V. (2013). Hierarchical Radial Basis Functions Networks. In *3D Surface Reconstruction* (pp. 77-110). Springer, New York.
- Boehler W., Marbs A. (2003). Investigating laser scanner accuracy. Institute for spatial information and surveying technology. University of Applied Sciences, Mainz, Germany.
- Chen S. (2012). Laser Scanning Technology for Bridge Monitoring, Laser Scanner Technology, Dr. J. Apolinar Munoz Rodriguez (Ed.), ISBN: 978-953-51-0280-9, InTech
- Chen, S. E., Liu, W., Bian, H., & Smith, B. (2014). 3D LiDAR Scans for Bridge Damage Evaluations. *Bridges*, 10, 9780784412640-052.
- Cheok G.S., Leigh S., Rukhin A. (2002). Calibration experiments of a Laser Scanner. *Building and Fire Research Laboratory, National Institute of Standards and Technology*, Gaithersburg, MD, USA.
- Gálvez, A., & Iglesias, A. (2012). Particle swarm optimization for non-uniform rational B-spline surface reconstruction from clouds of 3D data points. *Information Sciences*, 192, 174-192.
- Greaves T., Jenkins B. (2007). 3D laser scanning market red hot: 2006 industry revenues \$253 million, %43 growth, *SPAR Point Research*, LLC 5 (7).
- Hajian, H., Brandow, G. (2012). As-Built Documentation of Structural Components for Reinforced Concrete Construction Quality Control with 3D Laser Scanning. *Proceedings of the 2012 ASCE International Conference on Computing in Civil Engineering*. ASCE Publications, pp.253-260.
- Howlett, R. J., & Jain, L. C. (Eds.). (2001). *Radial basis function networks 1: recent developments in theory and applications* (Vol. 66). Springer.
- Kohonen, T. (2001). *Self-organizing maps* (Vol. 30). Springer Science & Business Media.
- Laflamme, S., & Connor, J. J. (2009, March). Application of self-tuning Gaussian networks for control of civil structures equipped with magnetorheological dampers. In *SPIE Smart Structures and Materials+ Nondestructive Evaluation and Health Monitoring* (pp. 72880M-72880M). International Society for Optics and Photonics.
- Laflamme, S., Slotine, J. J. E., & Connor, J. J. (2011). Wavelet network for semi-active control. *Journal of Engineering Mechanics*, 137(7), 462-474.

Laflamme, S., Slotine, J. E., & Connor, J. J. (2012). Self-organizing input space for control of structures. *Smart Materials and Structures*, 21(11), 115015.

Meng, Q., Li, B., Holstein, H., & Liu, Y. (2013). Parameterization of point-cloud freeform surfaces using adaptive sequential learning RBF networks. *Pattern Recognition*, 46(8), 2361-2375.

Meral C. (2011). Evaluation of Laser Scanning Technology for Bridge Inspection, MS Thesis, Civil Engineering Department, Drexel University

Mosalam, K. M., Takhirov, S. M., & Park, S. (2014). Applications of laser scanning to structures in laboratory tests and field surveys. *Structural Control and Health Monitoring*, 21(1), 115-134.

Olsen, M. J., Kuester, F., Chang, B. J., & Hutchinson, T. C. (2009). Terrestrial laser scanning-based structural damage assessment. *Journal of Computing in Civil Engineering*, 24(3), 264-272.

Olsen, M. J., Chen, Z., Hutchinson, T., & Kuester, F. (2013). Optical techniques for multiscale damage assessment. *Geomatics, Natural Hazards and Risk*, 4(1), 49-70.

Park, H. S., Lee, H. M., Adeli, H., & Lee, I. (2007). A New Approach For Health Monitoring Of Structures: Terrestrial Laser Scanning. *Computer aided civil and infrastructure engineering*, 22, 19–30.

Suresh, S., Narasimhan, S., & Sundararajan, N. (2008). Adaptive control of nonlinear smart base-isolated buildings using Gaussian kernel functions. *Structural Control and Health Monitoring*, 15(4), 585-603.

Trimble Inc. Trimble TX5 3D Laser Scanner User Guide. Online:
<http://mep.trimble.com/sites/mep.trimble.com/files/Trimble%20TX5%20User%20Guide.pdf>

Trimble Inc. Trimble TX5 Automation Interface User Guide. Online:
http://mep.trimble.com/sites/mep.trimble.com/files/marketing_material/Trimble_TX5_Automation_Interface.pdf

Wang, C., Shi, Z., Li, L., & Niu, X. (2012). Adaptive Parameterization and Reconstruction of 3D Face Images using Partial Differential Equations. *IJACT: International Journal of Advancements in Computing Technology*, 4(5), 214-221.

Werner T., Morris D. (2010). 3D Laser Scanning for Masonry Arch Bridges. *Proceedings of FIG Congress, Facing the Challenges – Building the Capacity*.

Wood, R. L., Hutchinson, T. C., Wittich, C. E., & Kuester, F. (2012). Characterizing Cracks in the Frescoes of Sala degli Elementi within Florence's Palazzo Vecchio. In *Progress in Cultural Heritage Preservation* (pp. 776-783). Springer Berlin Heidelberg.

Vosselman G. and Maas H.-G. *Airborne and Terrestrial Laser Scanning*, first ed. Whittles Publishing, Dunbeath, UK, 2010.

Xiong X., Adan A., Akinci B., and Huber D. Automatic creation of semantically rich 3D building models from laser scanner data, *Automat. Constr.*, 31: 325–337, 2013.

Zhang, Q., & Benveniste, A. (1992). Wavelet networks. *Neural Networks, IEEE Transactions on*, 3(6), 889-898.